

# UCSF

## UC San Francisco Previously Published Works

### Title

Pilot Study of Hyperpolarized  $^{13}\text{C}$  Metabolic Imaging in Pediatric Patients with Diffuse Intrinsic Pontine Glioma and Other CNS Cancers.

### Permalink

<https://escholarship.org/uc/item/43h6j5hd>

### Journal

AJNR. American journal of neuroradiology, 42(1)

### ISSN

0195-6108

### Authors

Autry, AW  
Park, I  
Kline, C  
[et al.](#)

### Publication Date

2021

### DOI

10.3174/ajnr.a6937

Peer reviewed

# Pilot Study of Hyperpolarized $^{13}\text{C}$ Metabolic Imaging in Pediatric Patients with Diffuse Intrinsic Pontine Glioma and Other CNS Cancers

A.W. Autry, I. Park, C. Kline, H.-Y. Chen, J.W. Gordon, S. Raber, C. Hoffman, Y. Kim, K. Okamoto, D.B. Vigneron, J.M. Lupo, M. Prados, Y. Li, D. Xu, and S. Mueller



## ABSTRACT

**BACKGROUND AND PURPOSE:** Pediatric CNS tumors commonly present challenges for radiographic interpretation on conventional MR imaging. This study sought to investigate the safety and tolerability of hyperpolarized carbon-13 ( $\text{HP-}^{13}\text{C}$ ) metabolic imaging in pediatric patients with brain tumors.

**MATERIALS AND METHODS:** Pediatric patients 3 to 18 years of age who were previously diagnosed with a brain tumor and could undergo MR imaging without sedation were eligible to enroll in this safety study of  $\text{HP [}^{13}\text{C]pyruvate}$ . Participants received a one-time injection of  $\text{HP [}^{13}\text{C]pyruvate}$  and were imaged using dynamic  $\text{HP-}^{13}\text{C}$  MR imaging. We assessed 2 dose levels: 0.34 mL/kg and the highest tolerated adult dose of 0.43 mL/kg. Participants were monitored throughout imaging and for 60 minutes postinjection, including pre- and postinjection electrocardiograms and vital sign measurements.

**RESULTS:** Between February 2017 and July 2019, ten participants (9 males; median age, 14 years; range, 10–17 years) were enrolled, of whom 6 completed injection of  $\text{HP [}^{13}\text{C]pyruvate}$  and dynamic  $\text{HP-}^{13}\text{C}$  MR imaging. Four participants failed to undergo  $\text{HP-}^{13}\text{C}$  MR imaging due to technical failures related to generating  $\text{HP [}^{13}\text{C]pyruvate}$  or MR imaging operability.  $\text{HP [}^{13}\text{C]pyruvate}$  was well-tolerated in all participants who completed the study, with no dose-limiting toxicities or adverse events observed at either 0.34 ( $n = 3$ ) or 0.43 ( $n = 3$ ) mL/kg.  $\text{HP [}^{13}\text{C]pyruvate}$  demonstrated characteristic conversion to  $\text{[}^{13}\text{C]lactate}$  and  $\text{[}^{13}\text{C]bicarbonate}$  in the brain. Due to poor accrual, the study was closed after only 3 participants were enrolled at the highest dose level.

**CONCLUSIONS:** Dynamic  $\text{HP-}^{13}\text{C}$  MR imaging was safely performed in 6 pediatric patients with CNS tumors and demonstrated  $\text{HP [}^{13}\text{C]pyruvate}$  brain metabolism.

**ABBREVIATIONS:** aSNR = apparent total SNR; EPSI = echo-planar spectroscopic imaging; DIPG = diffuse intrinsic pontine glioma;  $\text{HP-}^{13}\text{C}$  = hyperpolarized carbon-13

Pediatric brain tumors are the most commonly encountered solid tumors in childhood and now contribute to most cancer-related deaths in children.<sup>1</sup> Among these tumors, diffuse intrinsic pontine glioma (DIPG) poses the gravest threat, with the median overall survival in children being only 9 months from diagnosis, despite exhaustive research efforts.<sup>2</sup> In managing pediatric brain tumors, a key issue facing the neuro-oncology community is the

lack of imaging biomarkers that can support definitive and rapid assessment of response or resistance to treatment. While treatment response has traditionally been evaluated through MR imaging, there remain considerable challenges to radiographic interpretations of disease status. These potential shortcomings are exacerbated in the setting of novel therapies, such as immunotherapy, where there are no current standards to determine treatment effect versus disease progression based on imaging alone.

Because of the challenges in monitoring pediatric brain tumors using standard MR imaging, hyperpolarized carbon-13 ( $\text{HP-}^{13}\text{C}$ ) MR imaging presents a promising molecular methodology that

Received June 10, 2020; accepted after revision August 19.

From the Department of Radiology and Biomedical Imaging (A.W.A., H.-Y.C., J.W.G., Y.K., K.O., D.B.V., J.M.L., Y.L., D.X.); Division of Hematology/Oncology (C.K., S.R., C.H., M.P., S.M.), Department of Pediatrics; Departments of Neurology (C.K., S.M.), Bioengineering and Therapeutic Sciences (D.B.V.), and Neurological Surgery (D.B.V., M.P., S.M.); and UCSF/UC Berkeley Joint Graduate Group in Bioengineering (D.B.V., J.M.L., D.X.), University of California, San Francisco, San Francisco, California; and Department of Radiology (I.P.), Chonnam National University College of Medicine and Hospital, Gwangju, Korea.

A.W. Autry, I. Park, and C. Kline contributed equally to this work.

This study was supported by the Kure It-UCSF Grant for Underfunded Cancer Research (S.M.), as well as National Institutes of Health T32 Training Fellowship T32 CA151022 (A.W.A.) and P41 EB0341598 grants.

Please address correspondence to Duan Xu, MD, Department of Radiology and Biomedical Imaging, University of California, San Francisco, 1700 4th St, Room 303B, San Francisco, California 94158; e-mail: Duan.Xu@ucsf.edu

Indicates open access to non-subscribers at [www.ajnr.org](http://www.ajnr.org)

Indicates article with supplemental online tables.

<http://dx.doi.org/10.3174/ajnr.A6937>

can potentially extend current imaging capabilities. HP-<sup>13</sup>C MR imaging has enabled the noninvasive investigation of in vivo brain metabolism using molecular probes whose signal is transiently enhanced via dynamic nuclear polarization.<sup>3</sup> In studies of the adult brain,<sup>4-8</sup> intravenously injected HP [1-<sup>13</sup>C]pyruvate was shown to safely transport across the BBB and undergo enzymatic conversion to downstream metabolites [1-<sup>13</sup>C]lactate and [<sup>13</sup>C]bicarbonate, which serve as respective markers of glycolysis<sup>9</sup> and oxidative phosphorylation.<sup>10</sup> Given the metabolic alterations associated with cancer,<sup>11,12</sup> several of these imaging studies were designed to demonstrate the feasibility of HP-<sup>13</sup>C MR imaging in patients with gliomas<sup>4,5</sup> and also characterize serial imaging.<sup>8</sup> Kinetic modeling of serial data has most importantly shown evidence of aberrant metabolism in patients with progressive glioblastoma.<sup>8</sup> Additionally, earlier studies in patients with prostate cancer have indicated potential clinical relevance, based on the elevated ratio of [1-<sup>13</sup>C]lactate to [1-<sup>13</sup>C]pyruvate in biopsy-proved disease.<sup>13</sup>

Despite advances in the molecular characterization of pediatric brain tumors, development of imaging biomarkers has remained elusive.<sup>2</sup> Recent preclinical work evaluating [1-<sup>13</sup>C]pyruvate metabolism in human-derived orthotopic DIPG xenografts revealed that elevated levels of [1-<sup>13</sup>C]lactate could distinguish tumor from healthy brain stem tissue.<sup>14</sup> These data, derived from a disease model recapitulating human histopathology, provided evidence that HP-<sup>13</sup>C imaging may offer relevant metabolic biomarkers of central nervous system tumors.<sup>15</sup> Because DIPG lesions typically demonstrate only T2/FLAIR hyperintensity with little or no contrast enhancement in the weakly perfused environment of the brain stem,<sup>16</sup> these results are promising for a variety of pediatric brain tumors with similarly challenging radiographic presentations. In the setting of recurrent disease, in which standard MR imaging may not have distinct characteristics to confirm active disease versus treatment effect, such biomarkers could provide considerable value. They are also particularly relevant in the context of monitoring the efficacy of targeted treatment, as indicated by recent investigations of treatment response to histone deacetylase inhibitors in preclinical models of glioblastoma.<sup>17</sup>

The potential to identify tumor metabolism and biomarkers of treatment response combined with the preclinical and clinical support for HP [1-<sup>13</sup>C]pyruvate provided the basis for investigating the use of HP [1-<sup>13</sup>C]pyruvate in PNOC011, a “pilot study of safety and toxicity of acquiring HP-<sup>13</sup>C imaging in children with brain tumors” within the Pacific Pediatric Neuro-Oncology Consortium. The objectives of PNOC011 were to assess the safety and feasibility of HP-<sup>13</sup>C imaging in pediatric patients with brain tumors as a first step toward developing HP methodologies in this population. Herein, we describe our experience in PNOC011 using HP [1-<sup>13</sup>C]pyruvate in a dose-escalation study evaluating pediatric patients with a variety of brain tumors.

## MATERIALS AND METHODS

### Study Design

PNOC011 was an open-label, limited Phase I trial using a standard 3 + 3 design to assess the safety of the investigational imaging agent HP [1-<sup>13</sup>C]pyruvate across 2 dose levels in pediatric patients with brain tumors. Dose level 1 was 80% of the highest tolerated dose for adults (0.34 mL/kg). Dose level 2 was 100% of the highest

tolerated dose for adults (0.43 mL/kg). The intent of the study was to enroll a minimum of 3 participants per dose level and a total of 6 participants at the highest tolerated dose level.

### Participant Population

The single-center trial was conducted at the University of California, San Francisco, and designed to assess the safety and feasibility of HP [1-<sup>13</sup>C]pyruvate given intravenously for dynamic HP-<sup>13</sup>C MR imaging. Participants were recruited from the pediatric neuro-oncology clinic at the University of California, San Francisco, according to enrollment guidelines stipulating that subjects be 3–18 years of age and previously diagnosed with a brain tumor. Key inclusion criteria were a Karnofsky Performance Status Scale or Lansky Play-Performance Scale score of  $\geq 70$ ; no severe, uncontrolled medical illness; not pregnant or breastfeeding; use of effective contraception; and ability to provide informed consent. Key exclusion criteria included an inability to follow study procedures and a history or evidence of cardiac dysfunction. Any participant who was undergoing active anticancer therapy or on another investigational trial at the time of enrollment on PNOC011 was discussed with and approved by the study chair (S.M.). All participants and families provided informed consent or assent, as applicable, before initiation of protocol interventions.

This study was approved by the University of California, San Francisco institutional review board and the FDA under Investigational New Drug No. 131057 (S.M.). The trial was registered on clinicaltrials.gov under NCT02947373.

### Study Assessments

Before enrollment, participants underwent a complete neurologic examination, assessment of a performance score, evaluation of complete blood counts, liver function tests, and evaluation of electrolyte levels, as well as a baseline electrocardiogram. During and for 60 minutes after completion of the injection and imaging acquisition, the participant underwent continuous heart rate monitoring. Oxygen saturation and blood pressure were assessed every 15 minutes for a total of 60 minutes after completion of injection. An electrocardiogram was also repeated 60 minutes after the injection. Participants were contacted by the study team at 24 and 48 hours after completion of the injection to assess any toxicities related to HP [1-<sup>13</sup>C]pyruvate.

During the injection and imaging acquisition, a minimum of 2 pediatric advanced life-support-certified providers were present to monitor any acute events related to study procedures (C.K., C.H., S.R., S.M.).

### Study End Points

The primary end point of the study was safety based on the National Cancer Institute Common Terminology Criteria for Adverse Events, Version 4.0. Adverse events and serious adverse events were reported from the time of enrollment to 48 hours post-injection. Dose-limiting toxicities were defined as any HP [1-<sup>13</sup>C]pyruvate-related grade 2 or higher toxicity (excluding asymptomatic laboratory evaluations). Adverse events and serious adverse events were reviewed weekly by the study chair (S.M.) and the Pacific Pediatric Neuro-Oncology Consortium leadership (S.M., M.P.) per the Pacific Pediatric Neuro-Oncology Consortium

standardized operating procedures for safety review of clinical trials. The University of California, San Francisco Data Monitoring and Safety Committee monitored the trial.

The secondary end point was image quality, which was assessed qualitatively on the basis of descriptive characteristics only.

### **<sup>13</sup>C Hardware and Calibration**

All experiments were performed on a clinical 3T whole-body scanner (MR 750; GE Healthcare) equipped with 32-channel multi-nuclear imaging capability. Either an 8-channel bilateral paddle coil or a 32-channel head array coil with <sup>13</sup>C hardware configuration was used for optimal <sup>13</sup>C signal reception.<sup>18</sup> Transmit radiofrequency power was calibrated on a head-shaped phantom containing unenriched ethylene glycol (anhydrous, 99.8% HOCH<sub>2</sub>CH<sub>2</sub>OH; Sigma Aldrich).

### **Sample Polarization and Quality Control**

Dynamic nuclear polarization of [1-<sup>13</sup>C]pyruvate was performed using a 5T Spinlab polarizer (GE Healthcare) designed for clinical research applications.<sup>4</sup> To maintain an International Organization for Standardization 5 environment, pharmacists used an isolator (Getinge Group; Getinge 4-Glove Isolator Laminar Airflow, No. 2989; Getinge, France) and a clean bench laminar flow hood for the preparation of human [1-<sup>13</sup>C]pyruvate doses. Pharmacy kits filled with a mixture of 1.432-g [1-<sup>13</sup>C] pyruvic acid (Millipore Sigma) and a 28-mg electron paramagnetic agent (AH111501; GE Healthcare) were loaded into the Spinlab and polarized for at least 2.5 hours with 140-GHz microwave radiation at 5 T and 0.8 K. Following polarization, the pyruvate and trityl radical solution was rapidly dissolved in sterile water and passed through a filter under pressure to achieve a residual trityl concentration of <3 μM. This solution was then collected in a receiver vessel, neutralized, and diluted with a sodium hydroxide tris (hydroxymethyl) aminomethane/ethylenediaminetetraacetic acid buffer solution. An integrated quality control system rapidly measured the resulting pH, temperature, residual electron paramagnetic agent concentration, volume, pyruvate concentration, and polarization level. The solution passed through a terminal sterilization filter (Saint-Gobain PureFlo® D65R disc filter, 0.2 μm; Zenpure) before being collected in a Medrad syringe (Bayer HealthCare).

The quality control criteria for pharmacist release of the sample were the following: 1) polarization, ≥15%; 2) pyruvate concentration, 220–280 mM; 3) electron paramagnetic agent concentration, ≤3.0 μM; 4) pH, 5.0–9.0; 5) temperature, 25–37 °C; 6) volume, >38 mL; and 7) bubble point test on the sterilizing filter passed at 50 psi. The injected volume of HP[1-<sup>13</sup>C]pyruvate was based on a dosage of 0.34 mL/kg (dose level 1, *n* = 3) or 0.43 mL/kg (dose level 2, *n* = 3). The dose was delivered at a rate of 1–3 mL/s, less than the 5 mL/s used for adults, followed by a 20-mL sterile saline flush at the same rate.

### **Imaging Protocol**

Before imaging, a peripheral intravenous catheter was placed for administration of HP [1-<sup>13</sup>C]pyruvate. T2-weighted fast spin-echo images (TR/TE = 4000/60 ms, FOV = 26 cm, 192 × 256 matrix, 5-mm section thickness, and number of excitations = 2) acquired with the <sup>1</sup>H body coil served as an anatomic reference

for prescribing <sup>13</sup>C sequences. A 1-mL standard containing 8 mol/L of <sup>13</sup>C-urea was embedded in both 8- and 32-channel phased array receiver coils to provide an in vivo frequency reference for [1-<sup>13</sup>C]pyruvate:  $f_{\text{pyruvate}} = f_{\text{urea}} + 270 \text{ Hz}$ . On pharmacist approval of sample safety, participants were injected with HP [1-<sup>13</sup>C]pyruvate and imaged beginning 0–5 seconds after the saline flush by either dynamic <sup>13</sup>C EPI or echo-planar spectroscopic imaging (EPSI).

The EPI sequence (TR/TE = 62.5 ms/21.7 ms, FOV = 24 × 24 cm<sup>2</sup>, 8 slices, 20 time points, 3-second temporal resolution, 60-second acquisition time) was acquired with 3.38–4.50 cm<sup>3</sup> spatial resolution and offered whole-brain coverage (Online Table 1).<sup>19</sup> By means of spectral-spatial radiofrequency pulses, individual [1-<sup>13</sup>C]pyruvate, [1-<sup>13</sup>C]lactate, and [<sup>13</sup>C]bicarbonate resonances were sequentially excited over interleaved acquisitions with flip angles  $\alpha_{\text{pyruvate}}/\alpha_{\text{lactate}}/\alpha_{\text{bicarbonate}} = 20^\circ/30^\circ/30^\circ$ . In the case of EPSI (TR/TE = 130/6.1 ms, 24 time points, 3-second temporal resolution, 72-second acquisition time), single-section spectroscopic imaging data were acquired with a spatial resolution of 8 cm<sup>3</sup> and flip angles of 10° for all metabolites (Online Table 1).<sup>20</sup>

Two participants were repositioned after study protocol injection and HP-<sup>13</sup>C imaging for a short <sup>1</sup>H-MR imaging examination without gadolinium contrast using a 32-channel <sup>1</sup>H coil (Nova Medical, Wilmington, Massachusetts). This examination included 3D T1-weighted inversion recovery echo-spoiled gradient-echo images (TR/TE/TI = 6652/2448/450 ms, resolution = 1.5 × 1 × 1 mm<sup>3</sup>, FOV = 25.6 cm, matrix = 256 × 256), and 3D T2-weighted FLAIR images (TR/TE/TI = 6250/138/1702 ms, resolution = 1.5 × 1 × 1 mm<sup>3</sup>, FOV = 25.6 cm, matrix = 256 × 256). This imaging was performed to obtain quality proton images to overlay the carbon data.

### **Postprocessing of <sup>13</sup>C Data**

Dynamic EPI and EPSI <sup>13</sup>C data were processed according to previously described methods<sup>21</sup> and postprocessed to enhance the signal.<sup>22</sup> These data were then summed across time to display the total metabolite signal. The apparent total signal-to-noise ratio (aSNR) in the brain was computed by dividing the temporally summed metabolite signal, peak height values in the case of EPSI, by the SD of the noise outside the head.

## **RESULTS**

A total of 10 pediatric participants (9 males; median age, 14 years; range, 10–17 years) were enrolled (Table 1 and Online Table 2). Two additional participants consented to participate in the study but did not enroll (one due to disease progression and not returning to University of California, San Francisco for follow-up and the other due to changing his mind about participation). Due to technical issues related to generating HP [1-<sup>13</sup>C]pyruvate (*n* = 3) or MR imaging scanner operability (*n* = 1), 4 participants consented and enrolled, but did not undergo HP-<sup>13</sup>C MR imaging or injection of HP [1-<sup>13</sup>C]pyruvate. Details of the remaining 6 participants who underwent HP-<sup>13</sup>C MR imaging with injection of HP [1-<sup>13</sup>C]pyruvate can be found in Online Table 2 (5 males; median age, 14 years; range, 10–17 years). Diagnoses included DIPG (*n* = 3), pineoblastoma (*n* = 1), medulloblastoma (*n* = 1), and adamantinomatous craniopharyngioma (*n* = 1). Of these 6 participants, 3 were on active therapy at the time of HP-<sup>13</sup>C imaging. Following injection of HP

[1-<sup>13</sup>C]pyruvate, there were no adverse events in any participant at dose levels 1 or 2 based on assessments by supervising personnel and electrocardiogram and vital sign monitoring.

Table 2 provides the quality control measurements recorded for each dissolution of HP [1-<sup>13</sup>C]pyruvate before injection, including the delivered dosage volume (16–36 mL) and concentration (230–242 mM), with the time to injection ranging from 53 to 75 seconds.

Dynamic HP-<sup>13</sup>C imaging was successfully performed on participants using both the imaging- and spectroscopy-based acquisition schemes. Individual scan parameters are reported along with aSNR values from normal brain in Online Table 1. On the basis of the maximum aSNR that was calculated in the brain for each examination after applying signal-enhancement postprocessing techniques,<sup>22</sup> HP [1-<sup>13</sup>C]pyruvate (aSNR,  $7.85 \times 10^2 - 3.52 \times 10^5$ ), [1-<sup>13</sup>C]lactate (aSNR,  $1.75 \times 10^2 - 7.20 \times 10^4$ ), and [<sup>13</sup>C]bicarbonate (aSNR,  $64 - 1.52 \times 10^4$ ) were detectable across all participants (Online Table 1). Incidentally, each of the EPSI datasets was acquired with the paddle receiver coils, which allowed relatively high aSNR based on their proximity to the head.

Figure 1 shows HP-<sup>13</sup>C EPI data from a 9-year-old male participant (P-01) with DIPG, which have been overlaid on FLAIR images that demonstrated a hyper- and hypointense T2 lesion, indicated by

the yellow arrows. Temporally summed signal from <sup>13</sup>C-labeled metabolites provided evidence that HP [1-<sup>13</sup>C]pyruvate was transported across the BBB and subsequently underwent conversion to both [1-<sup>13</sup>C]lactate and [<sup>13</sup>C]bicarbonate. On the basis of visual inspection, the [1-<sup>13</sup>C]lactate signal in this anatomic lesion displayed a slight elevation relative to the normal-appearing contralateral brain stem (Fig 1, middle row). The same region is highlighted by the signal ratio map of [1-<sup>13</sup>C]lactate to [1-<sup>13</sup>C]pyruvate, which is free from the receive profile of <sup>13</sup>C hardware sensitivity (Fig 1, bottom row). At the time of study imaging, the patient was about 3 months from completion of radiation and undergoing therapy with convection-enhanced delivery with MTX110 (liquid panobinostat) coinjected with gadoteridol. Most interesting, on visual review of contrast-enhanced MR imaging of tumor regions previously treated with convection-enhanced delivery, the area of elevated lactate had not been reached with prior treatments.

Figure 2 displays HP-<sup>13</sup>C EPSI spectra from a 12-year-old male participant (P-02) with DIPG who was undergoing therapy with trametinib and everolimus. These HP-<sup>13</sup>C spectra are shown in relation to a FLAIR image demonstrating a T2-hyperintense lesion. Temporally summed <sup>13</sup>C spectra from a single section depict individual resonances of [1-<sup>13</sup>C]pyruvate, [1-<sup>13</sup>C]lactate, and [<sup>13</sup>C]bicarbonate (aliased from 160.8 ppm) throughout the inferior brain section (Fig 2A). Spectra from voxels corresponding with normal-appearing tissue (Fig 2B) and the lesion (Fig 2C) are annotated for metabolite reference. Due to the relatively large voxel size (8 cm<sup>3</sup>), some of the signal from Fig 2B is external to the brain, particularly in the case of [1-<sup>13</sup>C]alanine.

## DISCUSSION

Pediatric central nervous system tumors have historically presented challenges to radiographic interpretation of disease status on standard MR imaging, thereby prompting the exploration of alternative imaging strategies. Furthermore, current standard imaging frequently fails to adequately identify response or early treatment failure, particularly in the setting of developmental therapeutics, such as immunotherapy. PNOC011 demonstrated the tolerability of dynamic HP-<sup>13</sup>C metabolic imaging in pediatric participants with DIPG and other central nervous system tumors, while characterizing population-specific features of HP data. Injections of HP [1-<sup>13</sup>C]pyruvate were well-tolerated by all 6 participants without any reports of related adverse events. Based on the tolerance of HP [1-<sup>13</sup>C]pyruvate and the ability to detect conversion to downstream metabolites in real time, there is evidence that HP-<sup>13</sup>C techniques may inform about metabolism relevant to investigating pediatric DIPG and other brain malignancies.

**Table 1: Participant demographics**

Demographics	
Consented (n = 12)	
Age (median) (range) (yr)	14 (8–17)
Males (No.) (%)	10 (83)
Treatment (No. of patients)	
Completed protocol therapy	6
Eligible, withdrawn <sup>a</sup>	6
Completed <sup>13</sup> C injection (n = 6)	
Age (median) (range) (yr)	14 (10–17)
Males (No.) (%)	5 (83)
Diagnosis (anatomic location) (No.) (%)	
Diffuse intrinsic pontine glioma (pons)	3 (50)
Craniopharyngioma (suprasellar)	1 (17)
Medulloblastoma (posterior fossa)	1 (17)
Pineoblastoma (pineal gland)	1 (17)
Dose level (No. of patients)	
Dose level 1	3
Dose level 2	3
Safety (No. of events)	
Dose level toxicity	0
Adverse events	0

<sup>a</sup> Withdrawn due to the following: technical issue with MR imaging scanner (n = 1) or generating HP [1-<sup>13</sup>C]pyruvate (n = 3); change in participant choice to participate (n = 1); or disease progression before participation and participant did not return to University of California, San Francisco for follow-up treatment (n = 1).

**Table 2: Quality control for HP-<sup>13</sup>C injections**

Participant ID	EPA Conc. (μM)	[1- <sup>13</sup> C] Pyruvate Conc. (mM)	Volume Injected (mL)	Polarization (%)	Temp. (°C)	pH	Time to Injection (sec)
P-01	1.6	230	23.0	44.0	34.6	7.7	56
P-02	0.6	232	21.8	42.5	31.9	7.6	75
P-03	0.5	235	16.0	38.8	31.0	7.7	66
P-04	0.3	230	36.0	38.1	30.7	7.7	53
P-05	0.5	231	20.8	43.9	32.1	7.6	55
P-06	1.4	242	22.2	33.6	30.9	7.5	70

**Note:**—EPA indicates electron paramagnetic agent; Conc., concentration; Temp, temperature.



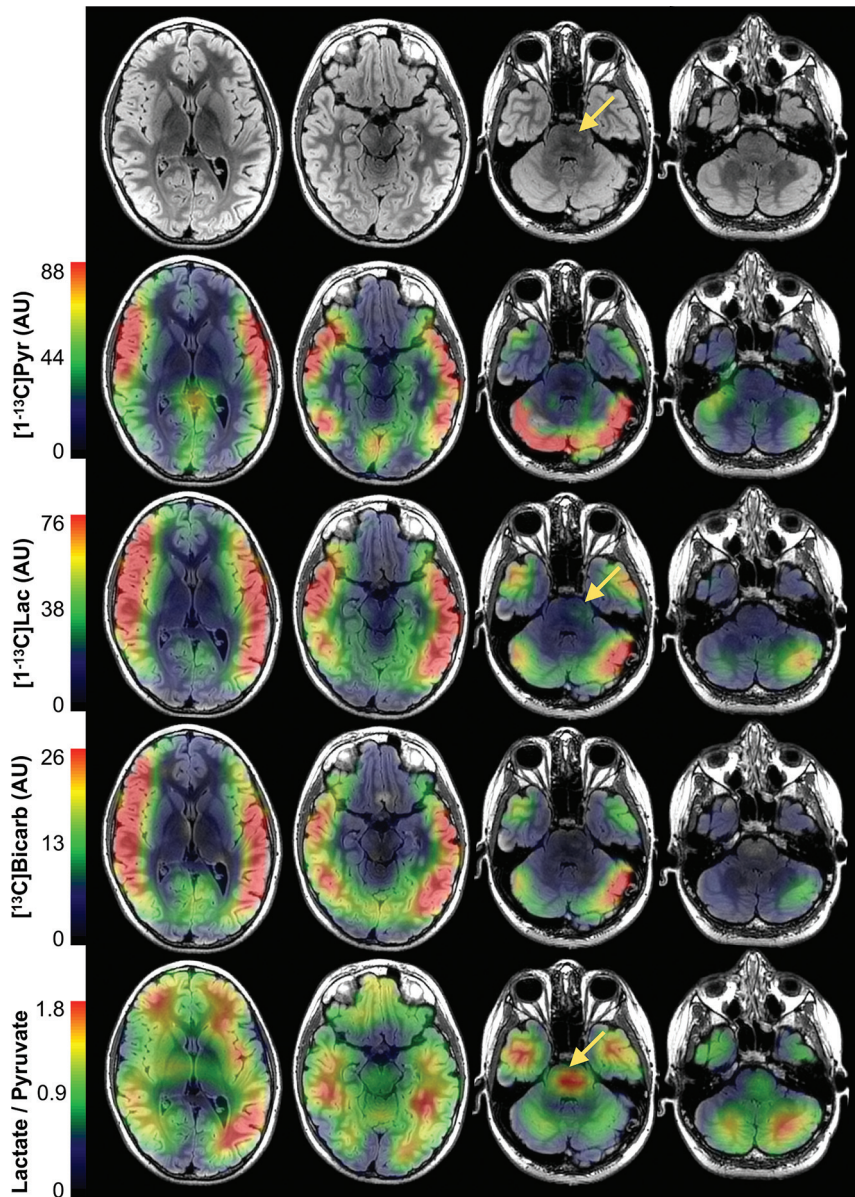


**FIG 1.** HP-<sup>13</sup>C imaging of DIPG. HP-<sup>13</sup>C EPI of a 9-year-old male participant (P-01) with DIPG following injection of HP [1-<sup>13</sup>C]pyruvate. Maps of the temporally summed signal from HP [1-<sup>13</sup>C]pyruvate and downstream metabolites [1-<sup>13</sup>C]lactate and [<sup>13</sup>C]bicarbonate are overlaid on <sup>1</sup>H FLAIR images, along with the ratio of [1-<sup>13</sup>C]lactate to [1-<sup>13</sup>C]pyruvate, which removes the shading of <sup>13</sup>C hardware sensitivity. Within the hyper- and hypointense T2 lesion indicated by the *yellow arrows*, there is a subtle increase in [1-<sup>13</sup>C]lactate signal relative to the normal-appearing contralateral brain stem. The ratio of [1-<sup>13</sup>C]lactate to [1-<sup>13</sup>C]pyruvate also demonstrates a local maximum in this anatomic lesion (*yellow arrow*). Pyr indicates pyruvate; Lac, lactate; Bicarb, bicarbonate; AU, arbitrary units.

Demonstrating the preliminary safety profile of HP-<sup>13</sup>C imaging in pediatric patients with a variety of CNS tumors represents a considerable advance with regard to translating this methodology to children. Within this population, the safety evaluation of HP [1-<sup>13</sup>C]pyruvate is of fundamental importance, and the experience thus far from the current study has matched the tolerability shown in adult brain studies.<sup>4-8</sup> In addition to the record of safety, this study was able to provide evidence that HP-<sup>13</sup>C imaging can capture metabolically relevant data. As reported in adults,<sup>4-8</sup> HP [1-<sup>13</sup>C]pyruvate displayed transport across the BBB and subsequent

conversion to [1-<sup>13</sup>C]lactate and [<sup>13</sup>C]bicarbonate over experimental time scales of approximately 60–72 seconds. Given the quality of these data, as measured by aSNR, HP-<sup>13</sup>C imaging appears to hold promise for investigating aberrant metabolism in pediatric brain tumors.

Several features of pediatric HP-<sup>13</sup>C imaging that were characterized in this study will inform the design of future clinical trials. Notably, children demonstrated more rapid delivery of HP [1-<sup>13</sup>C]pyruvate to the brain following injection compared with adults,<sup>4</sup> which is supported by the literature on their circulatory systems<sup>23</sup> and may also reflect higher monocarboxylate transporter activity.<sup>24</sup> This result has implications for HP-<sup>13</sup>C acquisitions because the kinetic modeling of [1-<sup>13</sup>C]pyruvate metabolism requires that the inflow of [1-<sup>13</sup>C]pyruvate be adequately sampled by imaging to quantify dynamic conversion. Thus, acquisitions should commence immediately following the completion of the injection. With respect to imaging of DIPG, the brain stem presented unique challenges because of its deep location in the head, which limited the detectability of <sup>13</sup>C signal by the receiver hardware. Freedom in positioning the paddle <sup>13</sup>C receivers helped reduce this issue by maximizing the proximity to the anatomic lesion;<sup>18</sup> however, other pediatric indications may benefit from custom-designed detector arrays that better conform to the surface of the head. While the spatial resolution was relatively low in this study (3.38–8 cm<sup>3</sup>), variable resolution acquisition strategies<sup>25</sup> and maintaining a short time to injection through quality control practices should greatly improve this issue.

One key limitation of this study was that only 3 participants were injected at the highest dose level. The initial study

intent was to enroll 6 participants at the highest tolerated dose to most accurately assess toxicity of this novel imaging technology in children and as per standard 3 + 3 statistical design. The failure to sufficiently enroll patients was largely due to the following: 1) limitations in enrolling pediatric patients who did not require anesthesia for brain imaging, 2) technical challenges that led to the failure of MR imaging or HP-<sup>13</sup>C injection (4 of 10 patients), and 3) coordinating MR research imaging with other standard-of-care imaging in an effort to limit the impact and stress on pediatric patients. Unfortunately, anesthesia has been shown to alter HP acquisitions

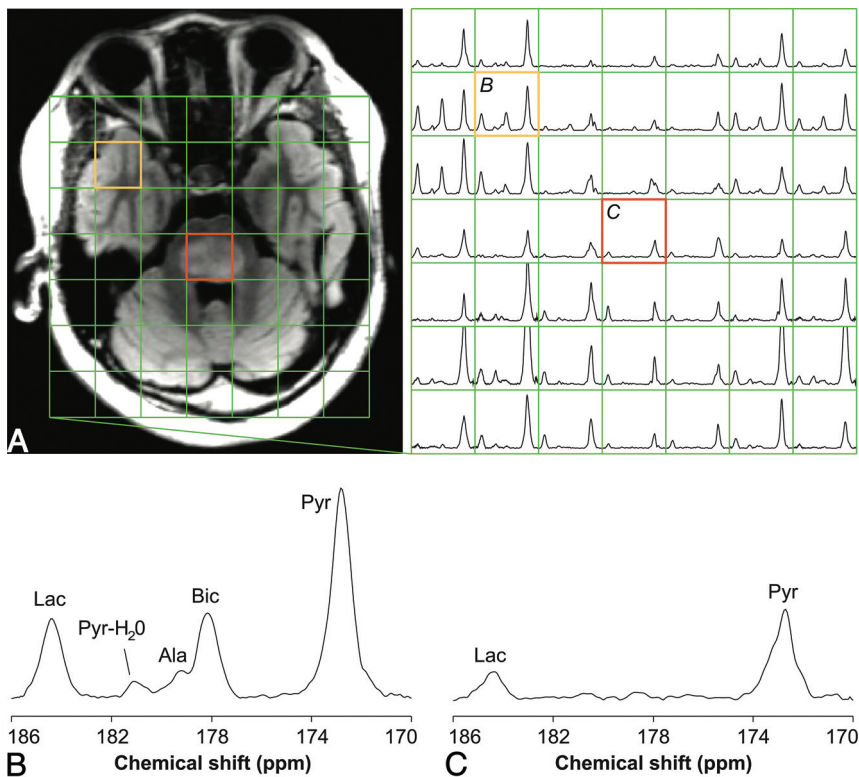


**FIG 2.** HP-<sup>13</sup>C spectroscopy of DIPG. HP-<sup>13</sup>C EPSI of a 12-year-old male participant (P-02) with DIPG following injection of HP [1-<sup>13</sup>C]pyruvate. Temporally summed <sup>13</sup>C spectra are shown together with their spatial correspondence to a <sup>1</sup>H FLAIR image from the center of the 2-cm-thick <sup>13</sup>C volume (A). Spectra from normal-appearing tissue (B) and the lesion (C) illustrate individual HP metabolite resonances. The [<sup>13</sup>C]bicarbonate resonance is aliased from 160.8 ppm. Pyr indicates [1-<sup>13</sup>C]pyruvate; Pyr-H<sub>2</sub>O, [1-<sup>13</sup>C]pyruvate-hydrate; Lac, [1-<sup>13</sup>C]lactate; Bic, [<sup>13</sup>C]bicarbonate; Ala, [1-<sup>13</sup>C]alanine exclusively from outside the brain.

in preclinical models, so this may be a confound for applying this technique in the youngest populations.<sup>26</sup> However, from a technical standpoint, injection-related failures can be overcome with evolving quality control procedures that preemptively address common issues.

Our group did identify particular challenges in the pediatric setting with regard to participation in nontherapeutic research studies because patients and families are already required to complete a large number of clinically relevant imaging and hospital visits. Such considerations in the pediatric setting must be taken into account for future imaging-based trials. One mechanism to potentially overcome these challenges would be to incorporate research imaging alongside interventional research studies. Another consideration for our trial is that we used weight-based volumes of metabolic contrast agent to facilitate consistent dosing across each dose level. While these volumes may display variability based on [1-<sup>13</sup>C]pyruvate mass, our study design remains aligned with what has been done in prior investigations of adults.<sup>4-8</sup>

Because effective therapeutic options for many pediatric brain tumors are limited, radiation therapy and experimental treatments, such as immunotherapy, frequently become standard-of-care options. As molecular characterization for pediatric brain tumors evolves and more individually tailored therapies become available in the future, pediatric neuro-oncology will need to

advance reliable imaging markers for evaluating response and resistance to treatment. From the results obtained in PNO011, HP-<sup>13</sup>C imaging may assist in developing imaging markers that reflect underlying brain metabolism and offer such insight.

## CONCLUSIONS

The safety and tolerability of dynamic HP-<sup>13</sup>C MR imaging with intravenously injected HP [1-<sup>13</sup>C]pyruvate in 6 pediatric patients with CNS tumors are very promising. Future studies with larger populations and options to incorporate HP-<sup>13</sup>C MR imaging alongside interventional studies will more comprehensively inform on the utility of HP-<sup>13</sup>C imaging for identifying imaging biomarkers.

## ACKNOWLEDGMENTS

We thank all the children and their families for their participation. We also thank the entire Pacific Pediatric Neuro-Oncology Consortium operation team for their support of the development and conduct of the study.

Disclosures: Adam W. Atry—RELATED: Grant: National Institutes of Health, Kure It-UCSF Grant for Unfunded Cancer Research, Comments: National Institutes of Health grant P41 EB0341598, Kure It-UCSF Grant for Unfunded Cancer Research\*; Other: National Institutes of Health/National Cancer Institute, Comments: T32 Training Fellowship T32 CA151022. Cassie Kline—UNRELATED: Grants/Grants Pending: Cannonball Kids cancer foundation, Frank A. Campini Foundation, National Institutes of Health KL2 Scholars Program. Hsin-Yu Chen—RELATED: Grant: National Institutes of Health, Kure It-UCSF Grant for Unfunded Cancer Research, Comments: This study was supported by the Kure It-UCSF Grant for Unfunded Cancer Research (S.M.) and the National Institutes of Health P41 EB0341598 grant.\* Yaewon Kim—RELATED: Grant: National Institutes of Health, Kure It-UCSF Grant for Unfunded Cancer Research, Comments: National Institutes of Health P41 EB0341598, Kure It-UCSF Grant for Unfunded Cancer Research.\* Janine M. Lupo—UNRELATED: Grants/Grants Pending: GE Healthcare, Comments: research funding.\* Michael Prados—RELATED: Grant: Kure It-UCSF Grant for Unfunded Cancer Research and University of California, San Francisco Comprehensive Cancer Center, Comments: nonprofit philanthropic group (Kure It-UCSF Grant for Unfunded Cancer Research), University of California, San Francisco Cancer Center: supplement grant (parent grant from the National Cancer Institute).\* Sabine Mueller—RELATED: Grant: Kure It-UCSF Grant for Unfunded Cancer Research, Comments: research grant to support the clinical trial. The foundation had no impact on the design or analysis.\* Duan Xu—RELATED: Grant: National Institutes of Health P41 EB0341598.\* \*Money paid to the institution.

## REFERENCES

- Ostrom QT, Gino C, Gittleman H, et al. **CBTRUS statistical report: primary brain and other central nervous system tumors diagnosed in the United States in 2012–2016.** *Neuro Oncol* 2019;21:v1–100 [CrossRef Medline](#)
- Cohen KJ, Heideman RL, Zhou T, et al. **Temozolomide in the treatment of children with newly diagnosed diffuse intrinsic pontine**



- gliomas: a report from the Children's Oncology Group. *Neuro Oncol* 2011;13:410–16 [CrossRef Medline](#)
3. Ardenkjaer-Larsen JH, Fridlund B, Gram A, et al. Increase in signal-to-noise ratio of >10,000 times in liquid-state NMR. *Proc Natl Acad Sci U S A* 2003;100:10158–63 [CrossRef Medline](#)
  4. Park I, Larson PEZ, Gordon JW, et al. Development of methods and feasibility of using hyperpolarized carbon-13 imaging data for evaluating brain metabolism in patient studies. *Magn Reson Med* 2018;80:864–73 [CrossRef Medline](#)
  5. Miloushev VZ, Granlund KL, Boltyanskiy R, et al. Metabolic imaging of the human brain with hyperpolarized <sup>13</sup>C pyruvate demonstrates <sup>13</sup>C lactate production in brain tumor patients. *Cancer Res* 2018;78:3755–60 [CrossRef Medline](#)
  6. Grist JT, McLean MA, Riemer F, et al. Quantifying normal human brain metabolism using hyperpolarized [1-<sup>13</sup>C]pyruvate and magnetic resonance imaging. *Neuroimage* 2019;189:171–79 [CrossRef Medline](#)
  7. Lee CY, Soliman H, Geraghty BJ, et al. Lactate topography of the human brain using hyperpolarized <sup>13</sup>C-MRI. *Neuroimage* 2020;204:116202 [CrossRef Medline](#)
  8. Autry AW, Gordon JW, Chen HY, et al. Characterization of serial hyperpolarized <sup>13</sup>C metabolic imaging in patients with glioma. *Neuroimage Clin* 2020;27:102323 [CrossRef Medline](#)
  9. Lunt YL, Vander Heiden MG. Aerobic glycolysis: meeting the metabolic requirements of cell proliferation. *Annu Rev Cell Dev Biol* 2011;27:441–64 [CrossRef Medline](#)
  10. Saraste M. Oxidative phosphorylation at the fin de siècle. *Science* 1999;283:1488–93 [CrossRef Medline](#)
  11. Warburg O. On respiratory impairment in cancer cells. *Science* 1956;124:269–70 [Medline](#)
  12. Ward PS, Thompson CB. Metabolic reprogramming: a cancer hallmark even Warburg did not anticipate. *Cancer Cell* 2012;21:297–308 [CrossRef Medline](#)
  13. Nelson SJ, Kurhanewicz J, Vigneron DB, et al. Metabolic imaging of patients with prostate cancer using hyperpolarized [1-<sup>13</sup>C]pyruvate. *Sci Transl Med* 2013;5:198ra108 [CrossRef Medline](#)
  14. Autry AW, Hashimuza R, James CD, et al. Measuring tumor metabolism in pediatric diffuse intrinsic pontine glioma using hyperpolarized carbon-13 MR metabolic imaging. *Contrast Media Mol Imaging* 2018;2018:3215658 [CrossRef Medline](#)
  15. Park I, Autry A, Chen Y, et al. Hyperpolarized carbon-13 metabolic imaging of pediatric patients with brain tumors: initial experience. In: *Proceedings of the Joint Meeting of the International Society for Magnetic Resonance in Medicine and the European Society for Magnetic Resonance in Medicine and Biology*, Paris, France. June 16–18, 2018
  16. Warren KE. Diffuse intrinsic pontine glioma: poised for progress. *Front Oncol* 2012;2:205 [CrossRef Medline](#)
  17. Radoul M, Najac C, Viswanath P, et al. HDAC inhibition in glioblastoma monitored by hyperpolarized <sup>13</sup>C MRSI. *NMR Biomed* 2019;32:e4044 [CrossRef Medline](#)
  18. Autry AW, Gordon JW, Carvajal L, et al. Comparison between 8- and 32-channel phased-array receive coils for in vivo hyperpolarized <sup>13</sup>C imaging of the human brain. *Magn Reson Med* 2019;82:833–41 [CrossRef Medline](#)
  19. Gordon JW, Chen HY, Autry AW, et al. Translation of carbon-13 EPI for hyperpolarized MR molecular imaging of prostate and brain cancer patients. *Magn Reson Med* 2019;81:2702–09 [CrossRef Medline](#)
  20. Larson PE, Bok R, Kerr AB, et al. Investigation of tumor hyperpolarized [1-<sup>13</sup>C]-pyruvate dynamics using time-resolved multiband RF excitation echo-planar MRSI. *Magn Reson Med* 2010;63:582–91 [CrossRef Medline](#)
  21. Crane JC, Gordon JW, Chen HY, et al. Hyperpolarized <sup>13</sup>C MRI data acquisition and analysis in prostate and brain at University of California, San Francisco. *NMR in Biomedicine* 2020 Mar 19. [Epub ahead of print] [CrossRef Medline](#)
  22. Chen HY, Autry AW, Brender JR, et al. Tensor image enhancement and optimal multichannel receiver combination analyses for human hyperpolarized <sup>13</sup>C MRSI. *Magn Reson Med* 2020 June 5. [Epub ahead of print] [CrossRef Medline](#)
  23. Wu C, Honarmand AR, Schnell S, et al. Age-related changes of normal cerebral and cardiac blood flow in children and adults aged 7 months to 61 years. *J Am Heart Assoc* 2016;5:e002657 [CrossRef Medline](#)
  24. Miranda-Goncalves V, Honavar M, Pinheiro C, et al. Monocarboxylate transporters (MCTs) in gliomas: expression and exploitation as therapeutic targets. *Neuro Oncol* 2013;15:172–88 [CrossRef Medline](#)
  25. Gordon JW, Autry AW, Tang S, et al. A variable resolution approach for improved acquisition of hyperpolarized <sup>13</sup>C metabolic MRI. *Magn Reson Med* 2020;84:2943–52 [CrossRef Medline](#)
  26. Josan S, Hurd R, Billingsley K, et al. Effects of isoflurane anesthesia on hyperpolarized <sup>13</sup>C metabolic measurements in rat brain. *Magn Reson Med* 2013;70:1117–24 [CrossRef Medline](#)